

# ON THE DESIGN OF AN ACTIVE AUXILIARY BEARING FOR ROTOR/MAGNETIC BEARING SYSTEMS

Iain S. Cade, M. Necip Sahinkaya, Clifford R. Burrows and Patrick S. Keogh

Department of Mechanical Engineering, University of Bath, UK

I.S.Cade@bath.ac.uk, M.N.Sahinkaya@bath.ac.uk, C.R.Burrows@bath.ac.uk, P.S.Keogh@bath.ac.uk

## ABSTRACT

This paper considers the design of an actively controlled auxiliary bearing system for use with magnetic bearings. During rotor/auxiliary bearing contact large frictional contact forces can lead to significant thermal stresses. Furthermore, the non-linear nature of the contact can induce unfavourable rotor dynamic behaviour. An active auxiliary bearing capable of reducing the contact forces and influencing the rotor dynamics during contact is proposed. Active auxiliary bearing design objectives include reducing the rotor/bearing contact forces during impact and influencing the rotor dynamics to prevent a trapped contact mode from becoming established. A piezo actuated system, using a closed hydraulic coupling, is presented. The dynamic performance of the actuators and hydraulic line are identified. In particular, the transfer function from actuator control signal to auxiliary bearing displacement is identified. Closed loop control of the active auxiliary bearing using local proportional-integral-differential control is also considered.

## INTRODUCTION

To prevent rotor/stator contact in a magnetic bearing system auxiliary bearings are present. During rotor/auxiliary bearing contact significant normal and tangential contact forces may occur. Furthermore, these forces may lead to localised thermal stresses [1]. The non-linear nature of the contact mechanics due to the auxiliary bearing may cause rotor instability after a contact event. Dynamic responses may include synchronous and asynchronous periodic contact [2, 3], sub-harmonic contact [4, 5], chaotic vibration [6], backwards whirl [7] and non-contacting rotor orbit. Furthermore, rotor drop may lead to transient rotor vibrations [8]. It is therefore important when designing a magnetic bearing system to consider both the operational life expectancy of the auxiliary bearing and the possible dynamic responses of the rotor after a contact event. Improvements in reducing the rotor/bearing contact forces may be achieved by changing the physical properties of the

auxiliary bearing. However, it is possible that this may increase the chance of undesirable rotor dynamics after a contact event. e.g. reducing the stiffness of the auxiliary bearing may reduce the contact force, but may also increase the contact duration and the occurrence of a constant rub orbit.

In principle, an actively controlled auxiliary bearing may be configured to reduce rotor/bearing contact forces and induce a desirable rotor orbit during and after a contact event. A hybrid piezo-hydraulic actuation system has been proposed by Palazzolo for control rotating machinery [9, 10]. Although this technique acts directly on the rotor, the high bandwidth and high forces associated with piezoelectric actuators are also favourable for active auxiliary bearing control. Piezoelectric actuators have further been used to control of flexible rotor by Alizadeh *et al.* [11, 12]. Improved rotor performance and reduced contact forces during rotor rub have been considered by Ulbrich *et al.* [13] and Jiang and Ulbrich [14].

This work considers the design of an actively controlled auxiliary bearing, which will allow the controller to reduce rotor/bearing contact forces and ensure desirable rotor dynamics.

## ROTOR/AUXILIARY BEARING CONTACT DYNAMICS

A rotor can be modelled in terms of a vector containing lateral and rotational displacements,  $\mathbf{x}_r(t)$ , at each node along the shaft. For a given force acting on the shaft the dynamics of the rotor can be expressed in terms of mass, stiffness, damping and gyroscopic terms  $\mathbf{M}_r$ ,  $\mathbf{K}_r$ ,  $\mathbf{C}_r$  and  $\mathbf{G}_r$ , respectively, as [15]

$$\mathbf{M}_r \ddot{\mathbf{x}}_r + (\Omega \mathbf{G}_r + \mathbf{C}_r) \dot{\mathbf{x}}_r + \mathbf{K}_r \mathbf{x}_r = \mathbf{F}_r \quad (1)$$

$\mathbf{F}_r(t)$  represents the forces acting on the shaft and may contain contact disturbance, control and contact forces,  $\mathbf{f}(t)$ ,  $\mathbf{u}(t)$  and  $\mathbf{d}(t)$ , respectively.  $\Omega$  corresponds to the rotor angular velocity. Rotor/auxiliary bearing contact will occur at node  $i$  if the displace-

ment of the rotor exceeds the clearance gap  $c^{(i)}$  as

$$\mathbf{d}^{(i)}(t) = \begin{cases} \mathbf{0} & \mathbf{x}_r^{(i)} - \mathbf{x}_b^{(i)} < c^{(i)} \\ \mathbf{z}_c(t) & \mathbf{x}_r^{(i)} - \mathbf{x}_b^{(i)} \geq c^{(i)} \end{cases} \quad (2)$$

where  $\mathbf{x}_b^{(i)}$  and  $\mathbf{x}_r^{(i)}$  represents the rotor and auxiliary bearing displacement at node  $i$ . Rotor/auxiliary bearing misalignment can also be accommodated in the bearing displacement.  $\mathbf{z}_c(t)$  is a vector containing the lateral and rotational contact forces acting on the rotor and is dependent on the contact force,  $f_c$ , and the dry sliding friction. A generalised rotor/auxiliary bearing contact force, for similar similar rotor/bearing materials, can be evaluated at node  $i$  using a Hertzian normal stress distribution [16]

$$\delta r_i - c_i = \frac{2(1 - \nu^2)}{\pi E L_i} \left( \frac{2}{3} + \ln \frac{16 R_i r_i}{l_i^2} \right) f_{ic}, \quad (3)$$

given that

$$l_i = 2.15 f_c^{1/2} \left( \frac{2 R_i R_i}{E L_i c_i} \right)^{1/2} \quad (4)$$

$R_i$  and  $r_i$  correspond to the shaft and auxiliary bearing outer and inner radii, respectively.  $L_i$  and  $l_i$  represent the auxiliary bearing axial length and contact arc length, respectively. The Young's modulus of the bearing and rotor are given by  $E$  and Poisson's ratio is specified by  $\nu$ . For an active auxiliary bearing the contact force  $f_c$  will depend on the auxiliary bearing actuators and control system used.

## ROTOR/ACTIVE MAGNETIC BEARING SYSTEM WITH ACTIVE AUXILIARY BEARINGS

The proposed rotor/magnetic bearing system consists of a 0.6 m long, 30 mm diameter rotor shaft. Small collars are located along the shaft at the auxiliary bearing locations to allow variation of the clearance gap from 0.4 to 0.75 mm. The total shaft mass with the auxiliary bearing collars and active magnetic bearing cores is approximately 6.5 kg. The rotor is supported by two eight pole active magnetic bearings with a maximum force capacity of 2.6 kN before roll-off at 275Hz. The active magnetic bearing/core clearance gap is 0.8 mm giving a negative stiffness of 3.9 MN/m. The bearings are orientated  $45^\circ$  from the vertical to maximize the static load capacity. Rotor position is measured using eddy current transducers positioned adjacent to the magnetic bearings. Initial rotor control is achieved using local proportional-integral-differential feedback of the rotor position relative to the magnetic bearing stators. Using proportional, integral and differential controller gains of 5.1 MN/m, 0.01 MNsm and

0.01 MNs/m, respectively, the first four, zero running speed, natural frequencies of the shaft are at 1049 rad/s (mainly rigid body), 1252 rad/s (mainly rigid body), 2329 rad/s (first flexible mode) and 4599 rad/s (second flexible mode).

## ACTIVE AUXILIARY BEARING SPECIFICATION

The objective is to minimise the rotor/auxiliary bearing contact force. However, to ensure system reliability the active auxiliary bearing is designed to be able to provide control forces during a contact event, similar to a passive rigidly mounted bearing. An upper limit of 10 kN has been specified as the maximum load capacity of the auxiliary bearing. This is sufficient to provide radial support, preventing rotor/stator contact, during base motion accelerations of 20g. During such contact events the impact duration is in the order of micro seconds. The bandwidth of the auxiliary should reflect this, hence, an upper frequency limit of 1 kHz is specified. The displacement of the auxiliary bearing should be as small as possible to prevent unnecessary rotor/bearing contact. An upper limit of 100  $\mu\text{m}$  has been chosen.

## ACTIVE AUXILIARY BEARING ACTUATOR DESIGN

To achieve the desired bandwidth, displacement and load capacity piezo actuators have been selected. However, piezo actuators can be damaged by shear load and sudden shock, hence, a hydraulic coupling is chosen between the piezo actuators and auxiliary bearing. This section details the actuator design including the piezo actuators, hydraulic line and the seal/plug.

### Piezoelectric Actuator

The displacement of a piezo actuator stack,  $x_a$ , can be specified in terms of its electric and mechanical properties as [17]

$$m_a \ddot{x}_a + c_a \dot{x}_a + k_a x_a = F_a + f_e \quad (5)$$

given that

$$F_a = T(v_{in} + v_c(q)), \quad q = T x + C(v_{in} + v_c(q)) \quad (6)$$

where  $m_a$ ,  $c_a$  and  $k_a$ , represent the actuator stack mass, stiffness and damping, respectively. The total charge across all the piezo ceramic elements and the electromechanical transform ratio are denoted by  $q$  and  $T$ , respectively. The force applied to the actuator from an external load is given by  $f_e$ . The actuator input voltage and the voltage drop across the stack, due to internal energy dissipation, are given

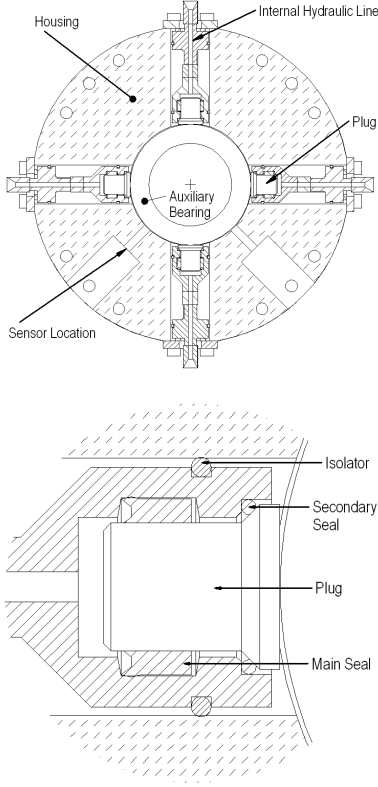


FIGURE 1: (a) Schematic drawing of the active auxiliary bearing assembly, (b) schematic drawing of the diaphragm.

by  $v_{in}$  and  $v_c(q)$ , respectively. The internal energy dissipation function  $v_c(q)$  leads to hysteresis in the open-loop operation of piezo electric actuators. However, in closed loop operation a near linear response from  $v_{in}$  to  $x_a$  can be achieved.

### Hydraulic Transmission Line Model

The change in pressure and volumetric flow rate along an element of a transmission line, assuming laminar flow, is a well understood topic [18]. For completeness a brief derivation of the dynamics is repeated here. The changes in pressure and volumetric flow rate are

$$\frac{\partial P}{\partial x} = -ZQ, \quad \frac{\partial Q}{\partial x} = -YP \quad (7)$$

where  $P$  and  $Q$  are the pressure and flow rates. Using equation (7) wave equations for the transmission line can be identified as

$$\frac{\partial^2 P}{\partial x^2} = ZYP, \quad \frac{\partial^2 Q}{\partial x^2} = ZYQ \quad (8)$$

where  $Z$  and  $Y$  are the impedance and admittance per unit length. The boundary conditions are  $x =$

$0; p = p_1; q = q_1$  and  $x = l; p = p_2; q = q_2$  where  $l$  is the length of the transmission line. Equations (8) can be solved as

$$P = \frac{(P_1 + Z_c Q_1)e^{-\Gamma x}}{2} + \frac{(P_1 - Z_c Q_1)e^{\Gamma x}}{2} \quad (9)$$

$$Q = \frac{(Q_1 + P_1/Z_c)e^{-\Gamma x}}{2} + \frac{(Q_1 - P_1/Z_c)e^{\Gamma x}}{2}$$

Here  $e^{\pm\Gamma x}$  corresponds to a wave propagating up/down the transmission line.  $\Gamma$  is the propagation constant given by  $\Gamma = \sqrt{ZY}$  and  $Z_c$  is the characteristic impedance,  $Z_c = \sqrt{Z/Y}$ . Given that  $\cosh(\alpha) = (e^\alpha + e^{-\alpha})/2$  and  $\sinh(\alpha) = (e^\alpha - e^{-\alpha})/2$  then equation (9) can be simplified as a matrix problem:

$$\begin{bmatrix} P \\ Q \end{bmatrix} = \begin{bmatrix} \cosh \Gamma x & -Z_c \sinh \Gamma x \\ -\frac{1}{Z_c} \sinh \Gamma x & \cosh \Gamma x \end{bmatrix} \begin{bmatrix} P_1 \\ Q_1 \end{bmatrix} \quad (10)$$

or at the end of the transmission line ( $x = l; p = p_2; q = q_2$ )

$$\begin{bmatrix} P_2 \\ Q_2 \end{bmatrix} = \begin{bmatrix} \cosh \Gamma l & -Z_c \sinh \Gamma l \\ -\frac{1}{Z_c} \sinh \Gamma l & \cosh \Gamma l \end{bmatrix} \begin{bmatrix} P_1 \\ Q_1 \end{bmatrix} \quad (11)$$

The ratio between input and output pressure can be expressed in the Laplace domain where  $\mathcal{L}[P_1(t)] = P_1(s)$ ,  $\mathcal{L}[P_2(t)] = P_2(s)$ ,  $\mathcal{L}[\Gamma(t)] = \Gamma(s)$ , as

$$\frac{P_2(s)}{P_1(s)} = \frac{1}{\cosh \Gamma(s)l + \frac{Z_c}{R_l} \sinh \Gamma(s)l} \quad (12)$$

given that for a lossless line model  $\Gamma(s) = s/c_0$  where  $c_0$  is the speed of sound in the medium.  $R_l = 128/\nu\pi r^4$  specifies the linearised resistance of a transmission line of diameter  $r$  containing a fluid with a viscosity  $\nu$ . The characteristic impedance  $Z_c$  is defined as  $Z_c = \sqrt{\beta_e \rho / \pi^2 r^4}$ , where  $\beta_e$  is the effective bulk modulus of the fluid within the transmission line and is a combined measure of both the compressibility of the fluid and the expansion of the hydraulic line. The effective bulk modulus for a flexible transmission line is

$$\beta_e = \left[ \frac{1}{\beta} + \frac{2}{E} \left( \frac{d_i^2 + d_o^2}{d_o^2 - d_i^2} + \mu \right) \right]^{-1} \quad (13)$$

where  $\beta$  is the bulk modulus of the fluid,  $E$  and  $\mu$  are the Young's modulus and Poisson's ratio of the pipe with internal and external diameters  $d_i$  and  $d_o$ , respectively. Equation (12) can be simplified using a Taylor series expansion terms of  $\cosh \Gamma(s)l$  and  $\sinh \Gamma(s)l$  with  $N$  terms. This is comparable to a lumped parameter approach breaking the transmission line in to  $N$  smaller sections. Equation (12) now

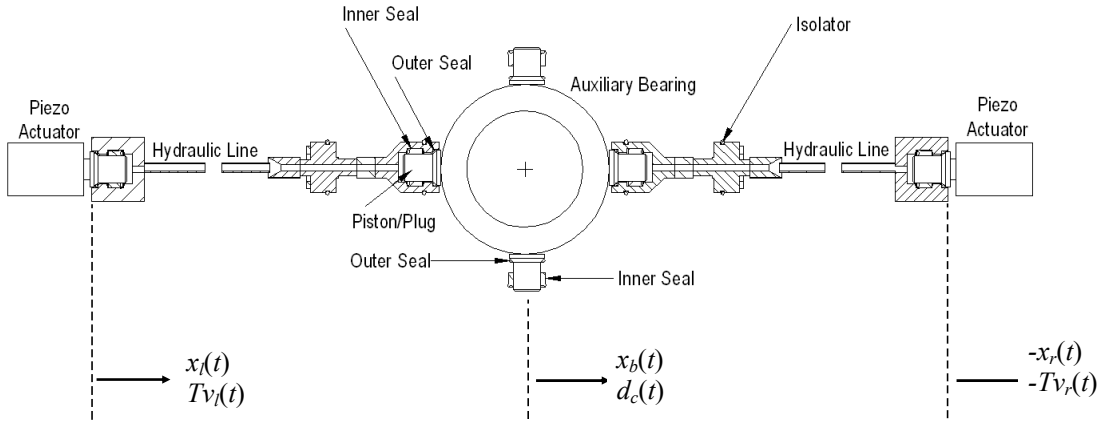


FIGURE 2: Active auxiliary bearing schematic showing horizontal piezo-hydraulic actuators

becomes:

$$\mathbf{T}_h(s) = \frac{1}{\sum_{n=0}^N \frac{(\Gamma(s)l)^{2n}}{(2n)!} + \frac{Z_c}{R_l} \sum_{n=0}^N \frac{(\Gamma(s)l)^{2n+1}}{(2n+1)!}} \quad (14)$$

where  $\mathbf{T}_h(s) = P_2(s)/P_1(s)$  is the transfer function from input pressure to output pressure across the closed hydraulic transmission line. It is noted that this method provides good agreement at lower frequencies, however, above the first few natural frequencies of the system significant errors may be present. In the context of this paper the objective is to design and use the hydraulic coupling at frequencies below the first natural frequency.

### Hydraulic Transmission Line Specification

The hydraulic transmission line can be separated into four different sections. These consist of the actuator/bearing piston chambers and the internal/external pipes. The performance of the transmission line in transferring pressure is dependent on its physical dimensions and also the hydraulic fluid. For this system a standard mineral oil has been specified. For systems requiring different dynamic performance characteristics other hydraulic fluids may provide improved performance.

Since the piezo-actuators and hydraulic fluid only provide control forces when acting in compression two hydraulic lines are required for each control axis. Therefore to move the auxiliary bearing in a plane normal to the rotor axis four actuators are required. To decouple orthogonal control axes the hydraulic lines are supported in the housing by rubber isolators. The compliance of the isolators can be specified in terms of stiffness and damping terms  $k_i$  and  $c_i$ , respectively.

Table 1 shows the dimensions and physical parameters of the hydraulic transmission line and the hydraulic fluid. For the dynamic model of the transmission line to be accurate laminar flow is required.

TABLE 1: Hydraulic transmission line parameters.

Parameter	Symbol	Value
Actuator chamber length	$l^{(a)}$	9 mm
Bearing chamber length	$l^{(b)}$	4 mm
Actuator chamber diameter	$l^{(a)}$	14 mm
Bearing chamber diameter	$l^{(b)}$	14 mm
Internal pipe length	$l^{(i)}$	70 mm
Internal pipe inner diameter	$d_p^{(i)}$	3 mm
Internal pipe outer diameter	$d_o^{(i)}$	5 mm
Internal pipe Poisson's ratio	$\mu$	0.34
Internal Young's modulus	$E$	104 GPa
External pipe length	$l^{(e)}$	350 mm
External pipe inner diameter	$d_p^{(e)}$	3.36 mm
External pipe outer diameter	$d_o^{(e)}$	4.8 mm
External pipe Poisson's ratio	$\mu$	0.25
External Young's modulus	$E$	210 GPa
Fluid bulk modulus	$\beta$	1.6 GPa
Fluid viscosity	$\nu$	0.003 Nsm <sup>-2</sup>
Fluid density	$\rho$	860 Kgm <sup>-3</sup>

For circular pipes a critical Reynolds number of 2400 is widely used, above which the flow becomes turbulent. For a maximum operating frequency of 1 kHz over a 100  $\mu$ m range the maximum velocity of the fluid is 0.016 m/s. For the hydraulic line specified this gives a Reynolds number of 1986. Each section of the hydraulic line was modelled using equation (14) limited to  $N = 10$ . The frequency response of the different sections of the hydraulic line and the whole line is shown in figure 5. The combined model, figure 5 (e), shows the first 4 natural frequencies before the Taylor expansion approximation becomes inaccurate, at approximately 3 kHz, above which confidence in the model is low. The specified auxiliary bearing bandwidth is 1 kHz. The model errors in-

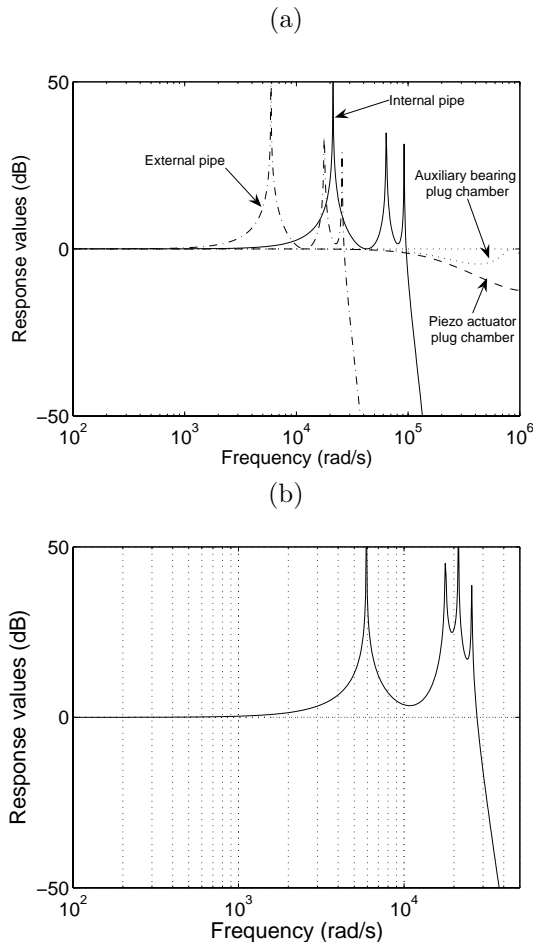


FIGURE 3: Active auxiliary bearing system transmission line frequency response. (a) Individual sections. (b) Full transmission line.

curred at high frequencies are above the maximum operating frequency of the system and allow for the performance to be predicted. The model also shows that the transmission line will operate below the first natural frequency. A system identification approach may also be undertaken to validate the model and identify higher frequency response characteristics.

### Seal Diaphragm

Two seals are present at each end of the hydraulic line to prevent fluid loss and allow displacement of the piston. A primary SKY type seal is positioned inboard and a secondary O-type is located outboard. The primary seal is housed in a deep groove to prevent movement. However, the groove edges are chamfered to permit the seal to deform allowing displacement of the piston. In this case the piston is a small plug (see figure 1). The secondary seal is positioned to provide both radial and axial stiffness (during compression). The addition of the secondary seal acting in compression, with respect to the con-

trol axis, allows a preload stiffness to be applied to the auxiliary bearing. This ensures the plug remains in contact with the auxiliary bearing during movement away from the hydraulic line.

The dynamics of the plug located by the seals can be expressed in terms of the plug mass,  $m_p$ , and combined seal stiffness and damping terms,  $k_s$  and  $c_s$ , respectively.

## ACTIVE AUXILIARY BEARING SYSTEM System Configuration

The piezo-hydraulic actuators only work in compression. Therefore two opposing actuators are required for each control axis. Hence, four piezo-hydraulic actuators, orientated at  $90^\circ$  to each other, are present at each auxiliary bearing (Figure 1). Two eddy current transducers are positioned at  $45^\circ$  to the piezo-hydraulic actuators to measure to auxiliary bearing displacement. To minimise the rotor/bearing sliding friction a rolling element type bearing, of mass 0.18 kg, has been chosen as the auxiliary bearing. The dynamics of the auxiliary bearing must be evaluated from the complete system.

TABLE 2: Hydraulic transmission line mechanical parameters.

Parameter	Symbol	Value
Combined seal stiffness	$k_s$	1 MN/m
Combined seal damping	$c_s$	500 Ns/m
Isolator stiffness	$k_i$	1 MN/m
Isolator seal damping	$c_i$	100 Ns/m
Piezo actuator mass	$m_a$	275 g
Piezo actuator stiffness	$k_a$	100 MN/m
Piezo actuator damping	$c_a$	324 Ns/m
Plug mass	$m_p$	25 g

### System Dynamics

Figure 2 shows a single active auxiliary bearing control axis. The complete active auxiliary bearing system dynamics be expressed as

$$\begin{bmatrix} X_l(s) \\ X_b(s) \\ X_r(s) \end{bmatrix} = \begin{bmatrix} T_{vl,xl}(s) & T_{dc,xl}(s) & T_{vr,xl}(s) \\ T_{dc,xl}(s) & T_{dc,xb}(s) & T_{dc,xr}(s) \\ T_{vr,xr}(s) & T_{vr,xb}(s) & T_{vr,xr}(s) \end{bmatrix} \begin{bmatrix} TV_l(s) \\ D_c(s) \\ TV_r(s) \end{bmatrix} \quad (15)$$

$X_b(s)$ ,  $X_l(s)$  and  $X_r(s)$  represent the Laplace transform of the auxiliary bearing, left piezo and right piezo actuator displacements, respectively.  $D_c(s)$ ,  $V_l(s)$  and  $V_r(s)$  correspond to the auxiliary bearing

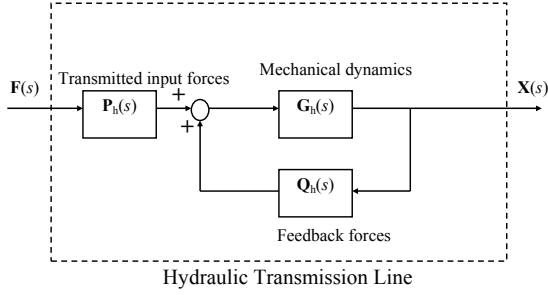


FIGURE 4: Block diagram showing hydraulic transmission model.

contact force and the left and right piezo actuator control voltages, respectively. Defining

$$\mathbf{F}(s) = \begin{bmatrix} TV_l(s) \\ D_c(s) \\ TV_r(s) \end{bmatrix}, \quad \text{and} \quad \mathbf{X}(s) = \begin{bmatrix} X_l(s) \\ X_b(s) \\ X_r(s) \end{bmatrix} \quad (16)$$

equation (15) can be expressed terms of the block diagram shown in figure 4 as

$$\mathbf{X}(s) = \mathbf{P}_h(s)\mathbf{G}_h(s) [\mathbf{I} + \mathbf{G}_h(s)\mathbf{Q}_h(s)] \mathbf{F}(s) \quad (17)$$

where  $\mathbf{G}_h(s)$ ,  $\mathbf{Q}_h(s)$  and  $\mathbf{P}_h(s)$  are the hydraulic transmission line mechanical dynamics, transmitted flow and pressure forces, respectively.

Figure 5 shows the frequency response of the different transfer functions  $T_{in,out}(s)$ . The response of the bearing to an actuator control force is shown to be flat up to the maximum required operating frequency with the first two natural frequencies occurring at 5926 and 17709 rad/s. The performance drop off above 3 kHz arises from truncation of the Taylor expansion used to model the transmission line.

### Impulse Response

The response of the system to an impulse disturbance, applied at either the auxiliary bearing or the piezo actuator, was simulated. An impulse disturbance force of 10 kN was chosen. The magnitude of this disturbance is comparable to large contact forces which may occur during a rotor/magnetic bearing system fault condition. The displacement of the auxiliary bearing and piezo-actuators is shown in Figure 6. The response of the bearing shows a maximum displacement of 58  $\mu\text{m}$ , before the bearing returns to its zero displacement location with zero overshoot. The transmitted forces through the hydraulic line cause small oscillations of the piezo actuators, approximately 10  $\mu\text{m}$ . The pressure ripples present in the opposing transmission lines act to cancel out vibration at the auxiliary bearing.

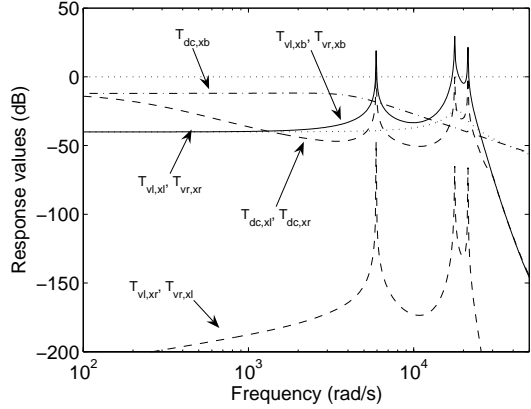


FIGURE 5: Active auxiliary bearing system frequency response.

The response of the system to an impulse, 10 kN, applied at a piezo actuator was also simulated. Figure 7 shows the displacements of the two actuators and the auxiliary bearing. The disturbed actuator is shown oscillating in a lightly damped manner. The transmitted force excites the bearing which is seen to oscillate with an amplitude of approximately 70  $\mu\text{m}$ . The undisturbed actuator shows very little displacement.

### CLOSED LOOP AUXILIARY BEARING CONTROL

The primary objective for an auxiliary bearing is to prevent rotor/stator contact. Closed loop control of the auxiliary bearing position can be used to ensure sufficient rotor/stator clearance is maintained for safe operation of an active magnetic bearing system. In this system two eddy current sensors are proposed to provide position feedback to an appropriate controller. Since the piezo-actuators and hydraulic transmission line can only provide control force in compression they are configured to operate as opposing pairs. i.e.  $v_l(t) + v_r(t) = v_{max}$ . Here  $v_{max}$  is the maximum control voltage applied to a piezo actuator and for zero error  $v_l(t) = v_r(t)$ . Control signals can be evaluated using local proportional-integral-differential (PID) feedback

$$U_c(s) = \left( \frac{g_i}{s} + g_p + \frac{g_d \omega_c s}{s + \omega_c} \right) X_b(s) \quad (18)$$

where  $U_c(s)$  represents the Laplace transform of the control signal.  $g_p$ ,  $g_i$ ,  $g_d$  and  $\omega_c$  are the proportional, integral, differential gains and cut-off frequency, respectively. The piezo-actuator control signals are

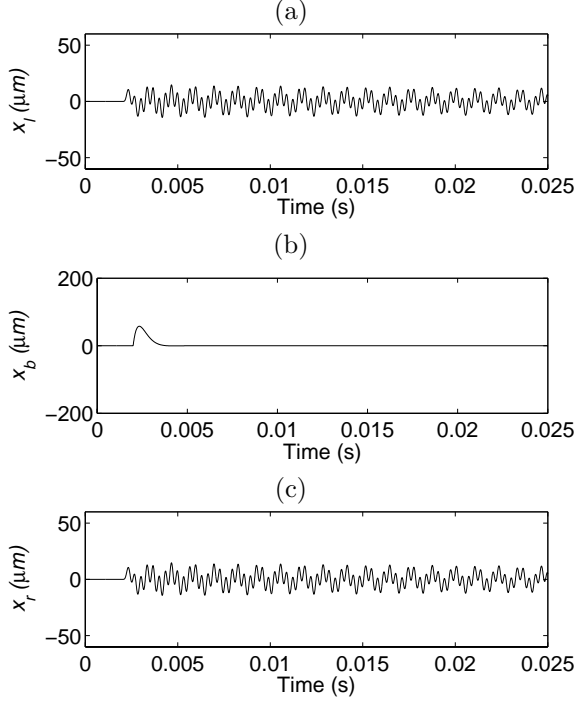


FIGURE 6: (a) Left hand side piezo actuator displacement. (b) Auxiliary bearing displacement. (c) Right hand side piezo actuator displacement.

therefore:

$$\begin{aligned} v_l(t) &= \frac{v_{max}}{2} + u_c(t)/T \\ v_r(t) &= \frac{v_{max}}{2} - u_c(t)/T \end{aligned} \quad (19)$$

where  $u_c(t)$  is the control signal and  $T$  is the electromechanical transform ratio. An impulse response of the PID controlled system was simulated. An impulse disturbance of 10 kN was applied at the piezo actuator. Controller gains were specified as  $g_p = 10$  kN/m,  $g_i = 1$  kN/ms,  $g_d = 0.9$  kNs/m and  $\omega_c = 1$  kHz. The displacements of the piezo actuators and auxiliary bearings are shown in figure 8 along with the demand control forces. It can be seen that compared to the uncontrolled case the displacement of the auxiliary bearing and the oscillation due to the hydraulic transmission line are both reduced. The control signals applied to the auxiliary bearings are shown in figure 8 (d).

## CONCLUSIONS

The design of an active auxiliary bearing for use in active magnetic bearing system has been presented. The active auxiliary bearing system consists of piezo actuators coupled to a rolling element bearing by hydraulic transmission lines. The dynamic performance of the piezo actuators and hydraulic transmission lines are considered. It is shown that for

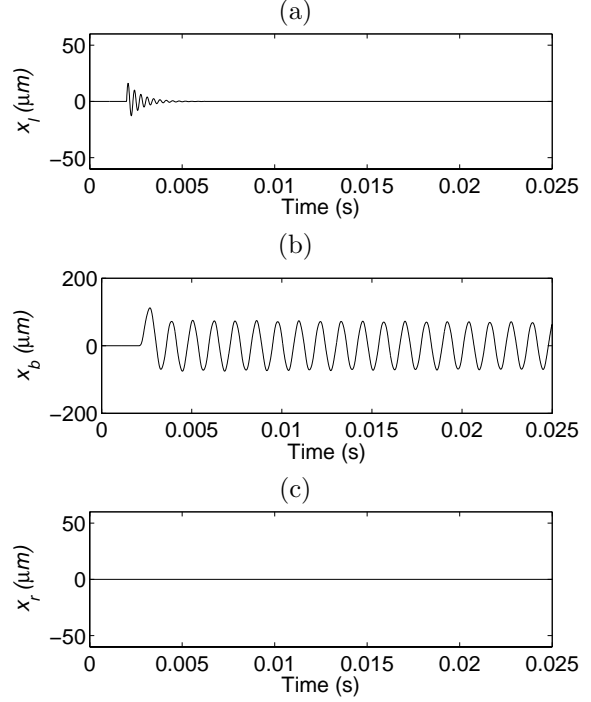


FIGURE 7: (a) Left hand side piezo actuator displacement. (b) Auxiliary bearing displacement. (c) Right hand side piezo actuator displacement.

the rotor specified sufficient control force and bearing frequency response can be achieved to prevent rotor/stator contact.

A system model of the active auxiliary bearing design is developed leading to the identification of the system transfer functions and dynamic behaviour. Simulations of the system response to an impulse disturbance were evaluated. Furthermore, closed loop control of the active auxiliary bearing system was simulated using PID feedback. It has been shown that closed loop control of the system can reduce both the magnitude of the initial displacement and subsequent oscillation of the auxiliary bearing.

## ACKNOWLEDGEMENT

The authors gratefully acknowledge the funding support of the Engineering and Physical Sciences Research Council through grant EP/D031389/1.

## REFERENCES

- [1] Keogh P.S. and Yong W.Y. "Thermal Assessment of Dynamic Rotor/Auxiliary Bearing Contact Events". *Journal of Tribology-Transactions of the ASME*, 129:143–152, 12007.
- [2] Keogh P.S. and Cole M.O.T "Rotor Vibration with Auxiliary Bearing Contact in Magnetic Bearing Systems - Part 1: Synchronous Dynamics". *Proceedings of the Institution of Mechanical Engineers*

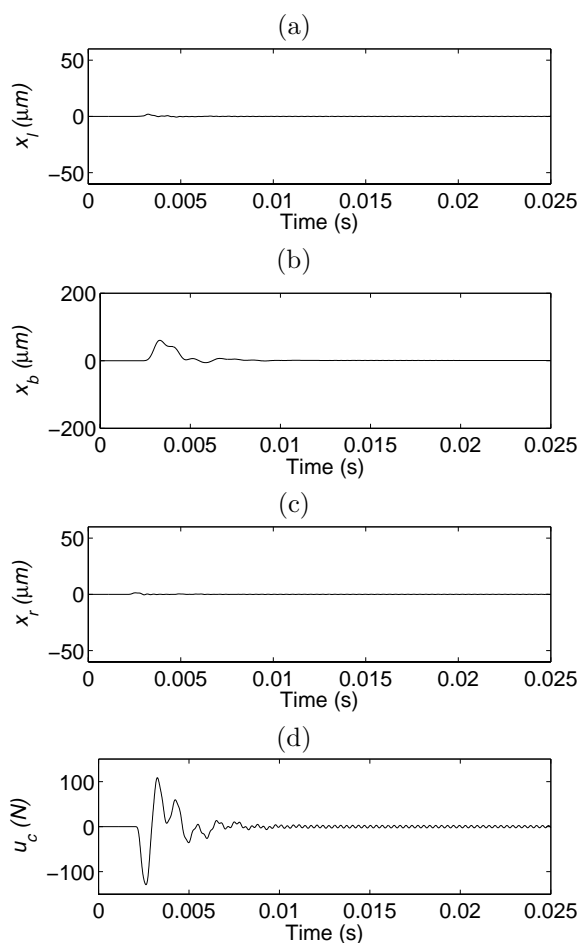


FIGURE 8: (a) Left hand side piezo actuator displacement. (b) Auxiliary bearing displacement. (c) Right hand side piezo actuator displacement. (d) Piezo actuator control force

*Part C-Journal of Mechanical Engineering Science*, 217(4):377–392, 2003.

- [3] Cole M.O.T. and Keogh P.S. “Asynchronous periodic contact modes for vibration within an annular clearance”. *Proceedings Institute of Mechanical Engineers Part C: Journal of Mechanical Engineering Science*, 217:1101–1115, 2003.
- [4] Ehrich F.F. “High Order Subharmonic Response of High Speed Rotors in Bearing Clearance”. *Journal of Vibration, Acoustics, Stress and Reliability in Design-Transactions of the ASME*, 10:9–16, 1988.
- [5] Childs D.W. “Rub Induced Parametric Excitation in Rotors”. *Transactions of the ASME, Journal of Mechanical Design*, 10:640–644, 1979.
- [6] Muszynska A. and Goldman P. “Chaotic Vibrations of Rotor/Bearing/Stator Systems with Looseness or Rubs”. *ASME Vibration and Noise Conference, Nonlinear Vibrations*, 54:187–194, 1993.
- [7] Bartha A.R. “Dry Friction Induced Backwards Whirl: Theory and Experiment”. *Proceedings of the 5th IFToMM Conference on Rotor Dynamics*, 757–767, 1998.
- [8] Ishii T. and Kirk G.R. “Transient Response Technique Applied to Active Magnetic Bearing Machinery During Rotor Drop”. *Journal of Vibration and Acoustics-Transactions of the ASME*, 118:154–163, 1996.
- [9] Palazzolo A.B., Lin R.R., Alexander A.F., Kascak R.M. and Montague J. “Piezoelectric Pushers for Active Vibration Control of Rotating Machinery”. *Transactions of the ASME, Journal of Vibration, Acoustics, Stress and Reliability in Design*, 111:298–305, 1989.
- [10] Palazzolo A.B., Lin R.R., Alexander A.F., Kascak R.M. and Montague J. “Test and Theory for Piezoelectric Actuator-Active Vibration Control of Rotating Machinery”. *Transactions of the ASME, Journal of Vibration and Acoustics*, 113:167–175, 1991.
- [11] Alizadeh A., Ehmann C., Schönhoff U., and Nordmann R. “Robust Active Vibration Control of Flexible Rotors Using Piezo Actuators as Active Bearing”. *ISCORMA 2, Gdańsk, Poland, 4-8 August, 2003*.
- [12] Alizadeh A., Ehmann C., Schönhoff U., and Nordmann R. “Active Bearing of Rotors Utilizing Robust Controlled Piezo Actuators”. *ASME Design Engineering Technical Conferences, Chicago, Illinois, USA, 2-6 September, 2003*.
- [13] Jiang J., and Ulbrich H. “Improvement of Rotor Performance Under Rubbing Conditions Through Active Auxiliary Bearings”. *The 10<sup>th</sup> International Symposium on Transport Phenomena and Dynamics of Rotating Machinery. ISCORMA 2, Gdańsk, Poland, 4-8 August, 2003*.
- [14] Ulbrich H., Chavez A., and Dhima R. “Minimization of Contact Forces in Case of Rotor Rubbing Using an Actively Controlled Auxiliary Bearing”. *The 10<sup>th</sup> International Symposium on Transport Phenomena and Dynamics of Rotating Machinery. Honolulu, Hawaii, 7-11 March 2004*.
- [15] Nelson H., and McVaugh J. “The Dynamics of Rotor-Bearing Systems Using Finite Elements”. *Journal of Engineering for Industry-Transactions of the ASME*, pp. 593–600. 1976.
- [16] Roark R.J. and Young W.C. *Formulas for Stress and Strain*. McGraw-Hill, New York, 1975.
- [17] Goldfarb M. and Celanovic N. “Modeling Piezoelectric Stack Actuators for Control of Micromanipulation”. *IEEE Control Systems*, pp. 593–600. 1976.
- [18] Watton J. *Fluid Power Systems: Modeling, simulation, analog and microcomputer control*. Prentice Hall, New York, 1989.